# A series of polyrotaxanes containing α-cyclodextrin and naphthalene-modified α-cyclodextrin and solvent effects on the fluorescence quenching by terminal units

**Makio Tamura,[a] De Gao[b] and Aihiko Ueno[a]**

[a] *Tokyo Institute of Technology, Department of Bioengineering, Graduate School of Bioscience and Biotechnology, 4259 Nagatsuta, Yokohama, 226-8501, Japan. E-mail: aueno@bio.titech.ac.jp; Fax: (+81)-45-924-5833*

[b] *Centro de Quimica Estrutural Complex 1, Instituto Superior Tecnica, Av. Rovisco Pais 1096, Lisboa Codex, Portugal. E-mail: degao1@yahoo.com*

***Received (in Cambridge, UK) 23rd January 2001, Accepted 3rd July 2001***
***First published as an Advance Article on the web 24th August 2001***

Photoquenching systems were constructed using polyrotaxanes in which cyclodextrin (CD) rings of α-CD and 6-deoxy-6-(-naphthalene-2-sulfonyl)-α-cyclodextrin (NpCD) are threaded by a poly(ethylene glycol) chain with trinitrophenyl (acceptor) units at both ends (**8**–**12**). The effects of the component ratio of the polyrotaxanes on the naphthalene fluorescence quenching efficiency and energy migration between naphthalene units were examined by steady-state and time-resolved spectra and anisotropy measurements. The quenching efficiency of **8**, which has the lowest content of NpCD, is larger than those of the polyrotaxanes with higher NpCD contents; however this tendency depends on the solvents. We explain the quenching mechanism of naphthalene fluorescence by the combination process of Förster type energy transfer and electron transfer to the trinitrophenyl units.

## Introduction

Photoinduced electron and energy transfer are fundamental processes in nature.[1,2] Heretofore, there has been a widespread interest in mimicking the natural photosynthesis process, which involves both energy transfer and electron transfer. As one approach, photon harvesting polymers have been studied, in which the capture of a photon by one chromophore in the polymer chain is followed by energy transfer among many chromophores to reach an energy acceptor.[3,4] This process is referred to as the antenna effect by Guillet and co-workers.[5] Recently, many dendrimer type light harvesting systems have been reported.[6,7] On the other hand, in a natural photosynthesis system, the components of the energy and electron transfer system are held together by weak non-covalent interactions that result in a spatially well-oriented arrangement. In connection with this, many supramolecular energy transfer[8–10] or electron transfer[11,12] systems, in which donor and acceptor components are linked by non-covalent interactions,[13] such as electric interaction,[8,11] hydrophobic bonding[9] and metal–ligand co-ordination,[10,12] have been investigated. In particular, rotaxane architecture has attracted interest for constructing artificial energy or electron systems.[13–15] We have reported on polyrotaxane type light harvesting antenna systems[15] to access the fundamental problem of whether the antenna effect becomes efficient when the number of absorption units increases.[7] In this case, there are only through space interactions between antenna chromophores, so it is possible to analyze the energy transfer efficiency without considering the effect of bond properties. These results indicated that the antenna effect becomes more noticeable with increasing number of the antenna unit in the polyrotaxanes. Here, we constructed polyrotaxane series composed of two different CD units: one is native α-CD and the other is naphthalene-modified α-CD (NpCD). In the polyrotaxanes, the rings of α-CD and NpCD are penetrated by poly(ethylene glycol) (approximate molecular weight = 2000) (PEG) bearing a trinitrophenyl moiety at both ends. The percentage of NpCD over the total CD units in the polyrotaxanes was varied to prepare polyrotaxanes with approximately 0%, 20%, 40%, 60%, 80% and 100.0% NpCD units (Scheme 1). The fluorescence intensities of naphthalene units in the polyrotaxane series are more efficiently quenched by the trinitrophenyl units when these are compared with the case of a mixed solution of NpCD and α,ω-trinitrophenyl terminated PEG. It was also observed that this quenching efficiency depends on the percentage of NpCD in the polyrotaxanes as well as on the solvent. Energy migration between the naphthalene chromophores was also investigated by an anisotropy method in propylence glycol (PG) at −70 °C. Time-resolved fluorescence decay was measured in various solvents to analyze what happened in these solvents, and we attempted to interpret naphthalene fluorescence quenching, particularly in the solvents containing high dielectric solvents such as MeCN, DMSO or formamide, by the combination of energy transfer and electron transfer from naphthalene to trinitrophenyl units.

## Results and discussion

### Preparation of polypseudorotaxanes

The polypseudorotaxanes were prepared by adding α,ω-diamino-PEG (diamino-PEG) (MW = 2000) into aqueous solutions of different ratios of naphthalene-modified NpCD and native α-CD. Here, the NpCD percentages over total CD units are 0%, 20%, 40%, 60%, 80% and 100%. In all cases, white precipitates appeared immediately. It is known that if diamino-PEG is added into native α-CD aqueous solution, polypseudorotaxane, in which α-CD rings are threaded by a diamino-PEG chain, is formed as white precipitate.[16] So we regarded the white precipitates formed in our study as polypseudorotaxanes, in which the CD rings of NpCD and α-CD were threaded by a diamino-PEG chain. The precipitates were collected and they were designated as **1**, **2**, **3**, **4**, **5** and **6** corresponding to 0%, 20%, 40%, 60%, 80% and 100% NpCD used as

 DOI: 10.1039/b100849h

**Table 1** Numbers of α-CD and NpCD and the percentages of NpCD in the polypseudorotaxanes[a]

| | 1 | 2 | 3 | 4 | 5 | 6 |
|---|---|---|---|---|---|---|
| Initial NpCD %[b] | 0.0 | 20.0 | 40 | 60.0 | 80.0 | 100.0 |
| $CD_{number}$[c] | 24.9 | 19.8 | 17.0 | 16.5 | 14.4 | 11.2 |
| $NpCD_{number}$[d] | 0.0 | 3.6 | 6.7 | 9.92 | 11.5 | 11.2 |
| NpCD %[e] | 0.0 | 18.2 | 39.4 | 60.1 | 79.9 | 100.0 |

[a–d] $^1$H NMR integral value is generally considered correct to within about 5% error. [a] The numbers of α-CD and NpCD were estimated from the $^1$H NMR spectra in the case where the approximate molecular weight of the PEG chain is 2000. These are measured at 25 °C in $D_2O$ solution, which contains a small amount of DMSO-$d_6$. [b] Initial NpCD content over total CD content when the polyrotaxanes were synthesized. [c] Number of total CD units in the polypseudorotaxanes. [d] Number of NpCD in the polypseudorotaxanes. [e] $NpCD_{number}/CD_{number} \times 100$ (%).

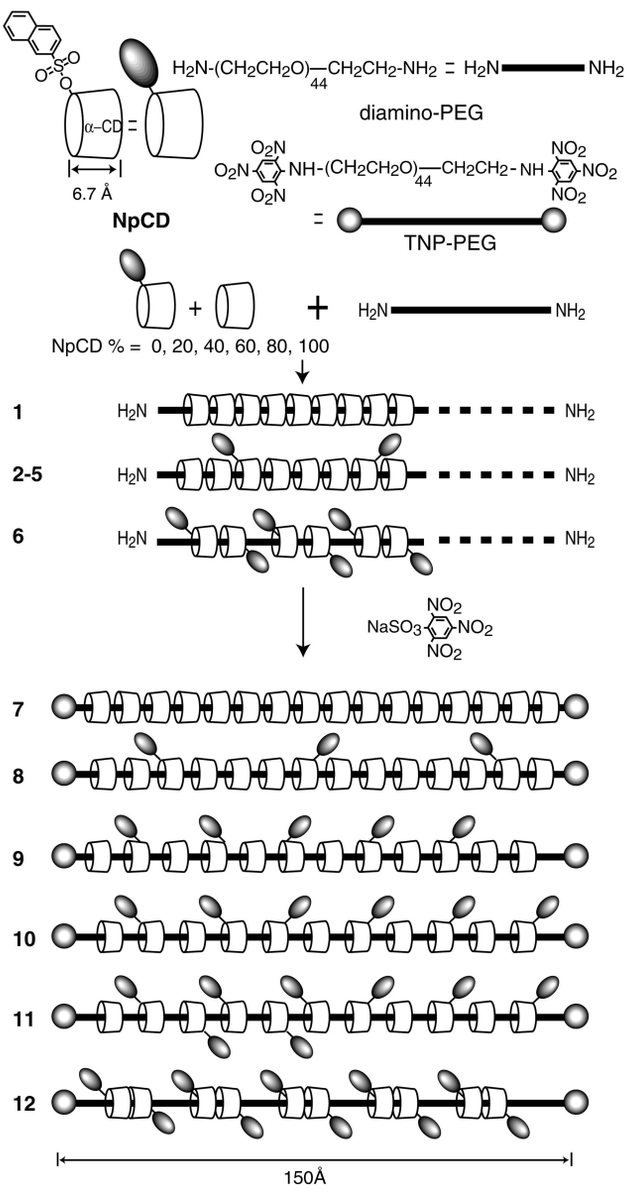


**Scheme 1**

starting percentages of NpCD. The $^1$H-NMR of **2** in $D_2O$ is shown in Fig. 1a and the composition data of the polyrotaxanes obtained by $^1$H NMR measurements are summarized in Table 1. The ratios of the NpCD in the polypseudorotaxanes are almost the same as its starting ratios. If there were some selectivity for CD or NpCD, or if some bias to concentrate CD

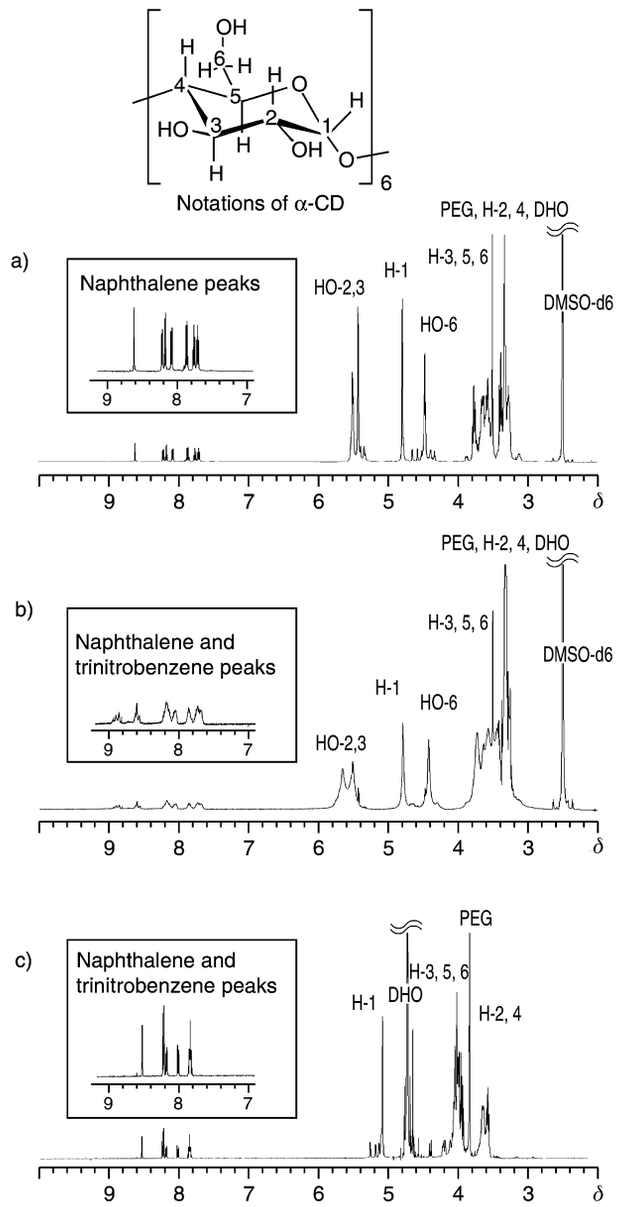


**Fig. 1** The $^1$H NMR spectra of **2** (a) and **8** (b) in DMSO-$d_6$, and **8** (c) in 1.5 M NaOD aqueous solution at 25 °C. Spectrum (c) was measured after **8** was dissolved in 1.5 M NaOD aqueous solution and kept at room temperature for 1.5 h.

or NpCD existed in the threading process, the percentages of NpCD over total CD units in the polyrotaxanes would not coincide with those in the starting mixture solutions. From these observations, we think that there is no selectivity for CD or NpCD in the threading process and the NpCD dispersions are uniform in the polypseudorotaxanes. The number of CD units decreases with increasing NpCD, as shown by the values of 24.6 for **1** and 11.2 for **6**. This result suggests that there exists remarkable steric hindrance between the naphthalene moiety and the neighboring CD unit in polypseudorotaxanes.

## Preparation of polyrotaxanes

The polypseudorotaxanes were converted into polyrotaxanes by the reaction of the amino groups of diamino-PEG in the polypseudorotaxanes with sodium 2,4,6-trinitrobenzene-1-sulfonate in aqueous buffer solution at pH 8.0 for 2 h. The trinitrophenyl moiety is large and consequently acts as a stopper to keep α-CD and NpCD in the polyrotaxanes.[17] Since the products of the reaction with 2,4,6-trinitrobenzene-1-sulfonate were insoluble in the aqueous solution, the products

were purified by washing with water and then with 5% ethanol in water to remove unreacted polypseudorotaxane and 2,4,6-trinitrobenzene-1-sulfonate. According to this procedure, polyrotaxanes **7**, **8**, **9**, **10**, **11** and **12** were prepared from **1**, **2**, **3**, **4**, **5** and **6**, respectively. All these polyrotaxanes were soluble in DMSO. The solubility in DMF is dependent on the composition, that is, **9**, **10**, **11** and **12** are soluble in DMF but the others are insoluble.

### NMR study of 7–12

The $^1$H NMR spectra of **7**–**12** in DMSO-$d_6$ show peaks corresponding to CD, diamino-PEG and the naphthalene unit (except for **7**), and the trinitrophenyl unit. For instance, the $^1$H NMR spectrum of **8** is shown in Fig. 1b. Although the $^1$H NMR spectra of the other polyrotaxanes are not shown here, all the polyrotaxanes exhibit similar spectral features; all peaks of the $^1$H NMR spectra are broadened, in contrast to polypseudorotaxanes **1**–**6** which exhibit sharp $^1$H NMR peaks in DMSO-$d_6$. This result may arise from the fact that movement of each component CD is restricted in **7**–**12**, closely packed as they are in the limited space between two stoppers, while the incorporated CD units can be dethreaded in **1**–**6** because of the absence of any stopper. Such $^1$H NMR peak broadening is consistent with the results reported for other polyrotaxanes.[14] To obtain further details we examined the 2D NOESY NMR spectrum of **7**, which exhibits $^1$H NMR peaks which are nicely separated from each other. The signals of C3-H and C5-H of α-CD show NOEs with the $CH_2$ of the diamino-PEG chain and this result seems reasonable because C3-H and C5-H are oriented toward the inside of the cavity of α-CD and most likely interact with the threading chain. In contrast, the signals of C1-H, C2-H and C4-H, which are located outside the cavity, do not show NOEs with the PEG chain. Furthermore, such NOEs were not observed for a mixture of α-CD and diamino-PEG in DMSO-$d_6$. The TLC data (*n*-BuOH–EtOH–water, 5 : 4 : 3 v/v/v) for **7**–**12** gave 0.00 as $R_f$ while **1**–**6** gave $R_f$ values of 0.30 (except for **6**) and/or 0.55 (except for **1**) that can be attributed to those of α-CD and NpCD, respectively. These data confirm that the CD units of **7**–**12** are mechanically interlocked on the PEG chain by the trinitrophenyl stoppers.

The ratio of NpCD and α-CD in the polyrotaxanes may be analyzed by comparing the $^1$H peak area of the naphthalene moiety with the area of the α-CD and the diamino-PEG chain. However, each of these peaks is too broad to make it possible to calculate the molar ratio correctly. Therefore, the large stoppers (trinitrophenyl) at the ends of **7**–**12** were removed by cleaving the bond with base (1.5 M NaOD solution) at room temperature to produce free CD units (Fig. 1c). The NMR peaks, which were broadened at first, became sharp after 1.5 h. These results indicate that each component of **7**–**12** is released from the supramolecular system under these conditions. After the reaction is completed, it is possible to compare the areas of the component $^1$H peaks. The results are summarized in Table 2. The percentages of NpCD in the polyrotaxanes **7**–**12** are almost the same as those of polypseudorotaxanes **1**–**6**. These results are also consistent with the elemental analysis data.

### Absorption spectroscopy of 7–12

The UV–vis absorption spectra of **7**–**12** in propylene glycol (PG) are shown in Fig. 2a and the absorption maximum ($\lambda_{max}$) and molecular coefficient ($\varepsilon$) values are collected in Table 3. Naphthalene absorption peaks were observed around 277, 313 and 327 nm and the trinitrophenyl absorption band was observed around 300–500 nm with two peaks around 350 and 417 nm. The molecular coefficient around 270–280 nm increases linearly and there is no spectral broadening or spectral shift with increasing number of NpCD in the polyrotaxanes. On the other hand, the absorbance and spectral shape of trinitrophenyl remain constant, which is the same as for the UV spectra of **7**. These results indicated that there was not strong electronic coupling among naphthalenes and between naphthalene and trinitrophenyl units in the ground state in PG. Fig. 2b shows the UV–vis absorption spectra of **12** in various solvents: PG, PG–acetonitrile (MeCN) 1 : 2, PG–*n*-butanol (BuOH) 1 : 2, PG–DMSO 1 : 2, PG–formamide 1 : 2. The absorbance around 280 nm in PG–BuOH 1 : 2 is a little smaller than that in PG, however above 300 nm, these two spectra are little different. In the other solvent mixtures, the shapes of the absorption spectra are almost the same as that in PG.

**Table 2** Numbers of CD and NpCD and the percentages of NpCD in the polyrotaxanes[a]

| | 7 | 8 | 9 | 10 | 11 | 12 |
|---|---|---|---|---|---|---|
| $CD_{number}$[b] | 15.7 | 13.8 | 11.7 | 11.4 | 10.5 | 9.9 |
| $NpCD_{number}$[c] | 0.0 | 2.8 | 4.7 | 6.4 | 8.4 | 9.9 |
| NpCD %[d] | 0.0 | 20.3 | 40.0 | 56.1 | 80.0 | 100.0 |
| MW[e] | 17700 | 16400 | 14700 | 14700 | 14200 | 14000 |

[a–d] $^1$H NMR integral value is generally considered correct to within about 5% error. [a] The number of α-CD and NpCD were estimated from the $^1$H NMR spectra measured at 60 °C in 1.5 M NaOD aq.–DMSO-$d_6$ (v : v = 1 : 1) solution. [b] Number of total CD units in the polyrotaxanes. [c] Number of NpCD units in the polyrotaxanes. [d] $NpCD_{number}/CD_{number} \times 100$ (%). [e] Molecular weights (MW) of the polyrotaxanes were estimated from $CD_{number}$ and $NpCD_{number}$ using the following equation: $972.85 \times (CD_{number} - NpCD_{number}) + 1163.07 \times (NpCD_{number}) + 2420.85$, where 972.85, 1163.07 and 2420.85 are the molecular weights of native α-CD, NpCD and diamino-PEG bearing a trinitrophenyl unit at both ends, respectively.

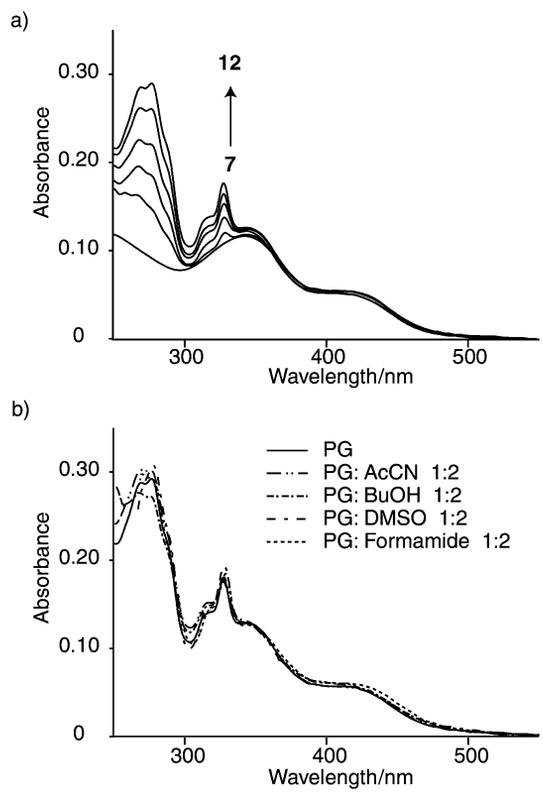


**Fig. 2** UV–vis absorption spectra of **7**–**12** in PG (a) and **12** in PG, PG–MeCN 1 : 2, PG–BuOH 1 : 2, PG–DMSO 1 : 2, PG–formamide 1 : 2 (b) at 25 °C. Concentration of each polyrotaxane is 1.8 μM.

### Steady-state fluorescence spectra

Figs. 3a and 3b show the steady-state fluorescence spectra ($\lambda_{ex}$ = 277, 327 nm) of **8**–**12** and the mixed solutions of NpCD and **7** in PG. The concentrations of the naphthalene and

**Table 3** Absorption extinction coefficients of polyrotaxanes **7**, **8**, **9**, **10**, **11** and **12**[a]

| nm | **7** $\varepsilon$/M$^{-1}$ cm$^{-1}$ | **8** $\varepsilon$/M$^{-1}$ cm$^{-1}$ | **9** $\varepsilon$/M$^{-1}$ cm$^{-1}$ | **10** $\varepsilon$/M$^{-1}$ cm$^{-1}$ | **11** $\varepsilon$/M$^{-1}$ cm$^{-1}$ | **12** $\varepsilon$/M$^{-1}$ cm$^{-1}$ |
|---|---|---|---|---|---|---|
| 277 | 38000 | 49000 | 62000 | 74000 | 87000 | 96000 |
| 327 | 36000 | 40000 | 46000 | 51000 | 55000 | 59000 |
| 350 | 40000 | 40000 | 41000 | 42000 | 42000 | 42000 |
| 417 | 17800 | 17800 | 17900 | 18000 | 18000 | 18000 |

[a] All parameters were recorded in propylene glycol at 25 °C.

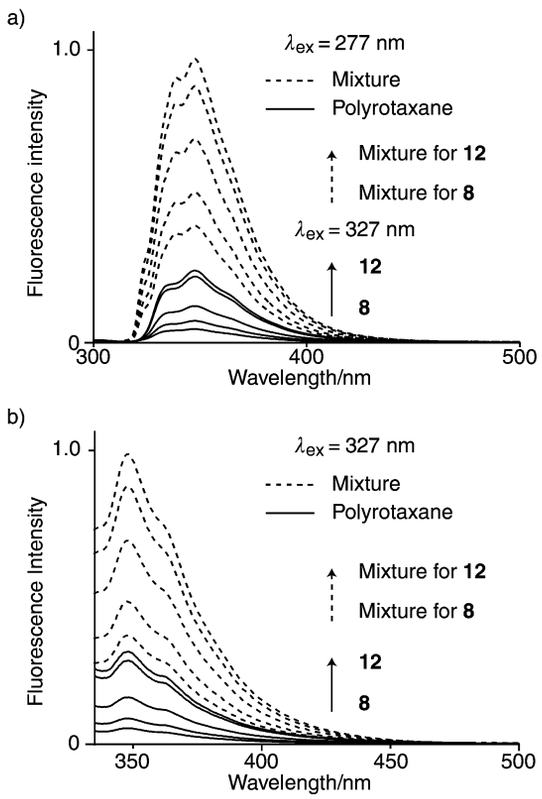


**Fig. 3** Steady-state corrected fluorescence emission spectra of polyrotaxanes **8**–**12** (0.6 μM) and the mixtures of **7** (0.6 μM) and NpCD in propylene glycol at 25 °C. Each mixture contains the same naphthalene unit as the corresponding polyrotaxane. Excitation wavelength was 277 nm (a), and 327 nm (b).

trinitrophenyl units in the mixed solutions were adjusted to become the same as those of the corresponding polyrotaxane solutions of **8**–**12**. The naphthalene fluorescence intensities of **8**–**12** ($\lambda_{em}$ = 347.5 nm) are smaller than those of the corresponding mixed solutions. The spectral shapes of **8**–**12** are virtually identical to those of mixed solutions and show no indication of naphthalene excimer emission around 400 nm, which means that the naphthalene units are strictly isolated from each other. There is a large spectral overlap between naphthalene fluorescence and trinitrophenyl absorbance, so excited energy on the naphthalene moiety can be transferred to the trinitrophenyl moiety by a dipole–dipole interaction (Förster type) mechanism.[18,19] This suggests that the energy transfer causes the naphthalene fluorescence quenching. However, there are many reports which show that nitrobenzene acts as an electron acceptor in fluorescence quenching *via* electron transfer.[20] Nevertheless, we found only one paper about electron transfer from naphthalene units to trinitrophenyl units, in which naphthalene and trinitrophenyl were adsorbed onto the surface of aerosil at high coverage.[21] In this paper, fluorescence from the charge transfer complex between naphthalene and trinitrobiphenyl was observed around 550 nm.

The quenching efficiency of the polyrotaxanes was estimated by comparing the naphthalene fluorescence intensity of polyrotaxanes at 347.5 nm ($\lambda_{ex}$ = 277 and 327 nm) ($I_{poly}$) with that of the corresponding mixed solutions ($I_{mix}$). Here we defined the fluorescence quenching efficiency (*QE*) as follows: *QE* (%) = (1 − $I_{poly}/I_{mix}$) × 100. The *QE* values of the polyrotaxanes in each solution are shown in Table 4. In PG, the highest quenching efficiency was observed for **8**, the values being 85.5% ($\lambda_{ex}$ = 327 nm) and 88.4% ($\lambda_{ex}$ = 277 nm), while the lowest quenching efficiency was observed for **12**, the values being 68.1% ($\lambda_{ex}$ = 327 nm) and 74.6% ($\lambda_{ex}$ = 277 nm). It is surprising that the most efficient antenna effect was observed in polyrotaxane **8**, which has the smallest number of naphthalene units in the polyrotaxane series, while the lowest quenching efficiency was observed for **12**.[15]

**Table 4** Quenching efficiency (%) calculated from steady-state fluorescence measurement (*QE*) and time-resolved fluorescence measurement ($E_q$) by the time-resolved fluorescence (%) of **8**–**12** and NpCD at 25 °C

| | PG | | | | |
|---|---|---|---|---|---|
| | **8** | **9** | **10** | **11** | **12** |
| *QE* ($\lambda_{ex}$ = 277 nm) | 88.4 | 85.5 | 82.2 | 74.3 | 74.6 |
| *QE* ($\lambda_{ex}$ = 327 nm) | 85.5 | 81.8 | 76.9 | 67.7 | 68.1 |
| $E_q$ | 21.4 | 22.9 | 22.9 | 24.2 | 27.1 |
| | PG–MeCN 1 : 2 | | | | |
| | **8** | **9** | **10** | **11** | **12** |
| *QE* ($\lambda_{ex}$ = 277 nm) | 63.5 | 54.4 | 50.2 | 42.9 | 32.8 |
| *QE* ($\lambda_{ex}$ = 327 nm) | 60.2 | 46.6 | 44.6 | 36.0 | 24.8 |
| $E_q$ | 4.78 | 1.89 | ~0.0 | 1.89 | ~0.0 |
| | PG–BuOH 1 : 2 | | | | |
| | **8** | **9** | **10** | **11** | **12** |
| *QE* ($\lambda_{ex}$ = 277 nm) | 67.6 | 62.1 | 62.9 | 62.2 | 64.1 |
| *QE* ($\lambda_{ex}$ = 327 nm) | 75.7 | 73.5 | 72.3 | 73.0 | 72.6 |
| $E_q$ | 11.9 | 13.4 | 13.4 | 14.9 | 14.9 |
| | PG–DMSO 1 : 2 | | | | |
| | **8** | **9** | **10** | **11** | **12** |
| *QE* ($\lambda_{ex}$ = 277 nm) | 69.4 | 41.4 | 35.6 | 36.7 | 35.0 |
| *QE* ($\lambda_{ex}$ = 327 nm) | 57.0 | 17.2 | 18.6 | 12.7 | 13.1 |
| $E_q$ | 16.0 | 16.0 | 16.0 | 16.0 | 16.0 |
| | PG–Formamide 1 : 2 | | | | |
| | **8** | **9** | **10** | **11** | **12** |
| *QE* ($\lambda_{ex}$ = 277 nm) | 56.1 | 42.8 | 40.6 | 35.7 | 23.0 |
| *QE* ($\lambda_{ex}$ = 327 nm) | 42.1 | 32.6 | 25.9 | 18.5 | 11.7 |
| $E_q$ | 17.5 | 17.5 | 15.8 | 17.5 | 15.8 |

The same quenching measurement was performed in the following solvents: PG–MeCN 1 : 2, PG–BuOH 1 : 2, PG–DMSO 1 : 2, PG–formamide 1 : 2. The fluorescence emission spectra of polyrotaxanes **9**–**12** are virtually identical to that of **8** in all solvents except for the PG–DMSO 1 : 2 solution, in which the fluorescence intensity around 425 nm slightly increases with increasing naphthalene content in the polyrotaxane. However, no clear excimer emission was detected in any of the solvents. Table 4 shows the *QE* values in all these solvents. It is interesting that in PG–BuOH 1 : 2 solvent, the *QE* values are almost constant, around 75% ($\lambda_{ex}$ = 327 nm) and 65% ($\lambda_{ex}$ = 277 nm) for all the polyrotaxanes. In contrast, the *QE* value drastically decreases with increasing content of naphthalene units when

**Table 5** Förster radius between NpCD and trinitrophenyl unit and between NpCD and NpCD in various solvents at 25 °C

| | NpCD–trinitrophenyl unit/Å | | NpCD–NpCD/Å |
|---|---|---|---|
| | $\lambda_{ex}$ = 277 nm | $\lambda_{ex}$ = 327 nm | $\lambda_{ex}$ = 277 nm |
| PG | 30.6 | 30.7 | 13.2 |
| PG–MeCN 1 : 2 | 28.7 | 28.5 | 12.3 |
| PG–BuOH 1 : 2 | 29.2 | 28.9 | 12.6 |
| PG–DMSO 1 : 2 | 25.6 | 24.6 | 11.2 |
| PG–formamide 1 : 2 | 29.3 | 29.2 | 12.4 |

**Table 6** Anisotropy of polyrotaxanes **8**–**12**, and NpCD (1.8 μM)

| **8** | **9** | **10** | **11** | **12** | NpCD |
|---|---|---|---|---|---|
| 0.144 ± 0.02 | 0.133 ± 0.02 | 0.091 ± 0.02 | 0.078 ± 0.01 | 0.060 ± 0.01 | 0.184 ± 0.01 |

All parameters were recorded in propylene glycol at −70 °C. $\lambda_{ex}$ = 277 nm and $\lambda_{em}$ = 348 nm.

the ratio of MeCN, DMSO, or formamide to PG increases. The Förster radii between naphthalene and trinitrophenyl units in PG, PG–MeCN 1 : 2, PG–DMSO 1 : 2, and PG–formamide 1 : 2 solvents are almost the same (Table 5). If energy transfer to the trinitrophenyl units is the only factor in quenching the naphthalene fluorescence, the tendencies of the *QE* values in PG–MeCN 1 : 2, PG–DMSO 1 : 2 and PG–formamide 1 : 2 solvents would be almost the same as that in PG. So, we consider that not only energy transfer but also electron transfer to trinitrophenyl units causes the quenching of the naphthalene fluorescence. This rationalizes the decrease of *QE* with increasing naphthalene content of the polyrotaxane; once the trinitrophenyl radical anion is generated by the electron transfer, it may no longer be able to quench the fluorescence of the other donor. The radical anion is more likely to be more stabilized in higher relative permittivity solvents like MeCN ($\varepsilon$ = 37.5), DMSO ($\varepsilon$ = 48.9) and formamide $\varepsilon$ = 111.0),[22] so in such solvents, the *QE* value decreases dramatically with increasing naphthalene content in the polyrotaxanes. In contrast, the radical anion would be less stable and more difficult to generate in the lower relative permittivity solvents such as PG ($\varepsilon$ = 32.0) and BuOH ($\varepsilon$ = 17.1). Also, especially in PG–BuOH 1 : 2 solvent, the influence of electron transfer may be very small.

Further measurement, such as transient absorption, is needed to prove the electron transfer phenomenon. However, we did not observe the absorption of the radical anion species of the trinitrophenyl unit; sufficient laser power to excite the naphthalene may not be available in our apparatus.

### Anisotropy study

We measured the anisotropy of naphthalene fluorescence at 348 nm ($\lambda_{ex}$ = 277 nm) in PG at −70 °C as a glass matrix. Under the conditions used, the fluorophore should remain stationary during the lifetime of the excited state, thereby effectively removing any depolarization effect due to fluorophore motion.[23] The degree of anisotropy $r$ is defined as $r = (I_{VV} - GI_{VH})/(I_{VV} + 2GI_{VH})$, where $I_{VV}$ and $I_{VH}$ are fluorescence intensities observed through a polarizer oriented parallel and perpendicular to the plane of polarization of the excitation beam, and $G$ is an instrumental correction factor.

If energy migration occurs and the absorption and emission do not involve the same chromophore, retention of anisotropy will be lost, resulting in a value of $r$ closer to zero. The anisotropy values of **8**–**12** are summarized in Table 6. It is clear that each anisotropy of the polyrotaxanes is smaller than that of NpCD, and the value decreases with increasing content of NpCD in the polyrotaxane. This indicates that energy migration occurs between the naphthalene units in the polyrotaxanes.

### Time-resolved measurements

The fluorescence lifetimes of the polyrotaxanes **8**–**12** and free NpCD were measured in the following solvents: PG, PG–MeCN 1 : 2, PG–BuOH 1 : 2, PG–DMSO 1 : 2, PG–formamide 1 : 2, using a time-correlated single photon counting instrument. Polyrotaxanes **8**–**12** and free NpCD were excited at 277 nm and the naphthalene fluorescence decay was monitored. The fluorescence decay data of free NpCD in all the solvents were well fitted by a double exponential decay function, and these cannot be fitted by a single exponential decay function. The values of the fluorescence lifetimes are given in Table 7. The results suggest that the naphthalene unit of free NpCD may be located in two different environments.[15] We attribute the shorter lifetime to the naphthalene unit which is located in the bulk solution apart from the CD unit, and the longer lifetime to the naphthalene units which may interact with the surface of the hydrophobic CD cavity. These arguments are consistent with the fact that naphthalene cannot be included in the α-CD cavity because of its larger size with respect to α-CD cavity. The lifetimes of shorter-lived species of free NpCD in all the solvents are almost the same (4.6–5.9 ns) except for PG–DMSO 1 : 2 solvent, in which the shorter lifetime is 1.9 ns. There may be unique electronic interaction between DMSO and naphthalene in the excited state to quench the fluorescence emission.

The fluorescence decay data of **8**–**12** in all the solvents can be well fitted by a double exponential decay function, and these cannot be fitted by a single exponential decay function. We attribute the shorter lifetime species of **8**–**12** to naphthalene units of the polyrotaxanes exposed to bulk solution, and the longer lifetime species to the naphthalene units located in the more hydrophobic environment produced by interaction with neighboring CD units and the PEG chain. It should be noted that the two fitted values for the lifetimes of the polyrotaxanes are just average values of naphthalene units located at the different positions of the polyrotaxanes, which may take many conformations. In all the solvents, the fraction of the longer lifetime species decreases with decreasing total CD content in the polyrotaxanes from **8** to **12**. This means that it becomes rather easier to hide the naphthalene units of the polyrotaxanes from the solvent with increasing total CD unit content in the polyrotaxanes. This tendency was observed in all the other solvents.

The quenching efficiency obtained by the time-resolved fluorescence measurement ($E_q$) could be evaluated from the average lifetime ($\tau$)[24] (Table 7) obtained from each lifetime species as eqn. (1), in which $\tau_i$ is the lifetime of each species and $a_i$ is the fraction of each species. If the rate constant of the

$$\tau = \frac{\sum_{i=1}^{N} a_i \tau_i}{\sum_{i=1}^{N} a_i} \quad (1)$$

**Table 7** Fluorescence lifetimes (ns) and average lifetimes (ns) of **8**–**12** and NpCD at 25 °C

| **8** | **9** | **10** | **11** | **12** | Free NpCD |
|---|---|---|---|---|---|
| PG | | | | | |
| 3.1 ± 0.01 (34.8%) | 3.0 ± 0.01 (35.4%) | 3.0 ± 0.01 (35.9%) | 3.0 ± 0.01 (36.3%) | 2.9 ± 0.01 (38.2%) | 5.9 ± 0.01 (94.6%) |
| 6.8 ± 0.03 (65.2%) | 6.7 ± 0.01 (64.6%) | 6.7 ± 0.01 (64.1%) | 6.5 ± 0.01 (63.7%) | 6.4 ± 0.01 (61.8%) | 26.3 ± 0.01 (5.4%) |
| $\chi^2 = 1.26$ | $\chi^2 = 1.18$ | $\chi^2 = 1.17$ | $\chi^2 = 1.10$ | $\chi^2 = 1.02$ | $\chi^2 = 1.14$ |
| Average lifetime | | | | | |
| 5.5 | 5.4 | 5.4 | 5.3 | 5.1 | 7.0 |
| PG–MeCN 1 : 2 | | | | | |
| 4.5 ± 0.01 (83.8%) | 4.7 ± 0.02 (86.2%) | 4.9 ± 0.01 (91.2%) | 4.9 ± 0.01 (94.0%) | 5.1 ± 0.01 (94.2%) | 4.7 ± 0.02 (94.2%) |
| 8.5 ± 0.02 (16.2%) | 8.6 ± 0.02 (13.8%) | 9.0 ± 0.01 (8.8%) | 9.2 ± 0.01 (6.0%) | 9.6 ± 0.01 (5.8%) | 14.3 ± 0.02 (5.8%) |
| $\chi^2 = 1.21$ | $\chi^2 = 1.27$ | $\chi^2 = 0.94$ | $\chi^2 = 1.07$ | $\chi^2 = 1.18$ | $\chi^2 = 1.23$ |
| Average lifetime | | | | | |
| 5.1 | 5.2 | 5.3 | 5.2 | 5.4 | 5.3 |
| PG–BuOH 1 : 2 | | | | | |
| 4.6 ± 0.01 (63.8%) | 4.6 ± 0.01 (64.4%) | 4.6 ± 0.01 (65.4%) | 4.6 ± 0.01 (65.8%) | 4.6 ± 0.02 (66.0%) | 5.9 ± 0.01 (94.7%) |
| 8.2 ± 0.01 (36.2%) | 8.1 ± 0.01 (35.6%) | 8.0 ± 0.02 (34.6%) | 7.9 ± 0.01 (34.2%) | 7.9 ± 0.02 (34.0%) | 21.2 ± 0.04 (5.3%) |
| $\chi^2 = 1.05$ | $\chi^2 = 1.16$ | $\chi^2 = 1.12$ | $\chi^2 = 1.17$ | $\chi^2 = 1.25$ | $\chi^2 = 1.19$ |
| Average lifetime | | | | | |
| 5.9 | 5.8 | 5.8 | 5.7 | 5.7 | 6.7 |
| PG–DMSO 1 : 2 | | | | | |
| 1.8 ± 0.01 (92.7%) | 1.9 ± 0.02 (95.1%) | 1.9 ± 0.01 (95.1%) | 1.9 ± 0.01 (95.5%) | 1.9 ± 0.01 (96.4%) | 1.9 ± 0.01 (95.1%) |
| 6.0 ± 0.03 (7.3%) | 6.0 ± 0.01 (4.9%) | 6.0 ± 0.01 (4.1%) | 6.0 ± 0.01 (4.5%) | 6.6 ± 0.01 (3.6%) | 14.3 ± 0.02 (4.9%) |
| $\chi^2 = 1.26$ | $\chi^2 = 1.18$ | $\chi^2 = 1.17$ | $\chi^2 = 1.10$ | $\chi^2 = 1.02$ | $\chi^2 = 1.01$ |
| Average lifetime | | | | | |
| 2.1 | 2.1 | 2.1 | 2.1 | 2.1 | 2.5 |
| PG–formamide 1 : 2 | | | | | |
| 4.3 ± 0.01 (95.5%) | 4.4 ± 0.02 (96.8%) | 4.5 ± 0.01 (96.9%) | 4.5 ± 0.01 (97.4%) | 4.6 ± 0.01 (97.4%) | 4.6 ± 0.01 (92.5%) |
| 13.2 ± 0.01 (4.5%) | 13.4 ± 0.03 (3.2%) | 13.5 ± 0.00 (3.1%) | 13.5 ± 0.01 (2.6%) | 13.8 ± 0.02 (2.6%) | 19.4 ± 0.02 (7.5%) |
| $\chi^2 = 0.84$ | $\chi^2 = 1.27$ | $\chi^2 = 1.00$ | $\chi^2 = 1.02$ | $\chi^2 = 1.18$ | $\chi^2 = 1.17$ |
| Average lifetime | | | | | |
| 4.7 | 4.7 | 4.8 | 4.7 | 4.8 | 5.7 |

radiative process ($k_f$) for naphthalene units is not changed in a different environment, the steady-state fluorescence ($I$) is proportional to the integral of each lifetime species represented as eqn. (2), and the $E_q$ value could be evaluated by eqn. (3),

$$I \propto \sum_{i=1}^{N} a_i \tau_i \tag{2}$$

$$E_q = (1 - (\tau'/\tau_n)) \times 100\% \tag{3}$$

where $\tau_n$ is the average lifetime without an acceptor (average value of NpCD) and $\tau'$ is the average lifetime quenched by an acceptor (average value of each polyrotaxane). For example, the $E_q$ value of **8** in PG (21.4%) is calculated using eqn. (4). The

$$\left(1 - \frac{5.5\ (\text{ns, average lifetime of } \mathbf{8})}{7.0\ (\text{ns, average of NpCD})}\right) \times 100 = 21.4\% \tag{4}$$

calculated quenching efficiency values ($E_q$) in PG, PG–MeCN 1 : 2, PG–BuOH 1 : 2, PG–DMSO 1 : 2, and PG–formamide 1 : 2 solvents are summarized in Table 4.

In contrast to the $QE$ values, the $E_q$ values for each polyrotaxane (**8**–**12**) are almost constant even in a solvent of higher relative permittivity such as PG–MeCN 1 : 2, PG–DMSO 1 : 2, and PG–formamide 1 : 2. In PG and BuOH solvents, $E_q$ values seem to slightly increase from **8** to **12**. This may mean that the energy and electron transfer efficiencies were almost the same in each polyrotaxane, and in some solvents, the energy and electron transfer efficiency was slightly accelerated with increasing naphthalene content. In steady-state fluorescence measurement, the change of the $S_1$ state population is zero [eqn. (5)]

$$\frac{d[S_1]}{dt} = 0 \tag{5}$$

and in this equation, the radical anion of the trinitrophenyl unit generated by electron transfer prevents the quenching of naphthalene fluorescence, so in higher dielectric solvents, the $QE$ value decreases with increasing naphthalene content in the polyrotaxane. However, the result of time-resolved fluorescence measurement reflects the initial energy and electron transfer process, and for this reason, the tendency of the $E_q$ value may be different from that of $QE$. The $E_q$ values seem to be smaller than $QE$ in each solvent. The experimental limitation for the very fast decay component by time-resolved measurement may reflect this difference.[24]

### Energy transfer mechanism

The energy transfer mechanism can be shown as follows:

D* + A ⟶ D + A* (D is donor and A is acceptor)

From this viewpoint, the rate constant for energy transfer is given by eqn. (6), where $H_{DA}^{ET}$ is the electronic coupling between

$$K_{ET} = (2\pi/h)(H_{DA}^{ET})^2 FC \tag{6}$$

the two excited states exchanged in the energy transfer process and $FC$ is an appropriate Frank–Condon factor. The electronic factor $H_{DA}^{ET} = \langle \Psi_{D^*,A} | (e^2/R) \Psi_{D,A^*} \rangle$ is a two-electron matrix element involving the HOMOs and LUMOs of the energy donor and energy acceptor centers. This factor can be split into two additive terms a coulombic term and an exchange term, and each of them can become the predominant factor depending on the energy transfer system and situation. The coulombic (resonance, dipole–dipole, Förster) mechanism does not require physical contact between donor and acceptor and the mechanism for singlet–singlet energy transfer is interpreted in terms of the coulombic mechanism, which involves a long distance dipole–dipole interaction. The exchange (Dexter) mechanism is a short–range mechanism that requires orbital overlap between donor and acceptor. Due to the exponential fall-off of donor–acceptor orbital overlap, the rate constant of Dexter mechanism energy transfer is expected to fall off with distance exponentially. In general, the Dexter mechanism is applied to explain triplet–triplet energy transfer. The relationship between

**Table 8** Fluorescence quantum yield ($\phi$) of NpCD in various solvents at 25 °C

| | $\lambda_{ex}$ = 277 nm | $\lambda_{ex}$ = 327 nm |
|---|---|---|
| PG ($n$ = 1.432) | 0.158 ± 0.001 | 0.158 ± 0.001 |
| PG–MeCN 1 : 2 ($n$ = 1.378) | 0.093 ± 0.003 | 0.088 ± 0.002 |
| PG–BuOH 1 : 2 ($n$ = 1.410) | 0.113 ± 0.002 | 0.104 ± 0.003 |
| PG–DMSO ($n$ = 1.462) | 0.159 ± 0.003 | 0.047 ± 0.002 |
| PG–formamide 1 : 2 ($n$ = 1.442) | 0.125 ± 0.002 | 0.121 ± 0.003 |

the rate constant ($k_{ET}$) for Förster type energy transfer and the spectroscopic and photophysical properties of the two molecular components is given by the classical Förster formula eqn. (7), where $N$ is Avogadro's number, and $R$ is the distance

$$k_{ET} = \frac{9000(\ln 10)k^2 \phi J}{128\pi^5 n^4 N\tau R^6} \quad (7)$$

between the centers of the two dipoles for the donor and acceptor molecules. The Förster radius ($R_0$), where the energy transfer efficiency is 50% between donor and acceptor, can be obtained by eqn (8), where $k^2$ is the molecular orientation

$$R_0 = 8.785 \times 10^{-25} k^2 \phi n^{-4} J \quad (8)$$

factor, which is 3/2 in random distribution between the donor and acceptor, $\phi$ is the fluorescence quantum yield of the donor in the absence of an acceptor, and the measured $\phi$ values of NpCD in various solvents; PG, PG–MeCN 1 : 2, PG–BuOH 1 : 2, PG–DMSO 1 : 2, PG–formamide 1 : 2, are summarized in Table 8. $n$ is the refractive index of the solvent, and $J$ is the overlap integral between the fluorescence spectrum of the donor and the absorption spectrum of the acceptor. The overlap integral $J$ is given by eqn. (9), where $F_D$ is the relative fluor-

$$J = \int F_D(v)\, \varepsilon_A(v) v^{-4} \mathrm{d}v \quad (9)$$

escence intensity of the donor normalized on the wavenumber scale ($v$) and $\varepsilon_A(v)$ is the excitation coefficient of the acceptor at the wavenumber. The calculated Förster radius ($R_0$) values between naphthalene and trinitrophenyl units at excitation wavelengths 277 and 327 nm are summarized in Table 5. From this estimation, if the naphthalene and trinitrophenyl units are separated by the same distance in different solvents, the order of the $k_{ET}$ values in these solvents is as follows: PG, PG–formamide 1 : 2 > PG–BuOH 1 : 2 > PG–MeCN 1 : 2 > PG–DMSO 1 : 2. The relationship between energy transfer efficiency ($E_t$) and the distance between donor and acceptor ($R$) was given by eqn. (10) using the Förster radius ($R_0$).

$$E_t = \frac{R_0^6}{R_0^6 + R^6} \quad (10)$$

In the polyrotaxanes, naphthalene units may be distributed uniformly on the axial PEG chain, whose length is about 150 Å in the extended form. Fig. 4 shows the theoretical curves of energy transfer against the distance $R$ between 0 and 70 Å, which is about half of the PEG chain length and about the maximum distance between naphthalene and trinitrophenyl units, in each solvent at excitation wavelength 277 nm. The average energy transfer efficiency between naphthalene and trinitrophenyl units ($ET_{N-T}$) over these distances is estimated by using eqn. (11). $ET_{N-T}$ of $\lambda_{ex}$ = 277 and 327 nm in the solvents

$$ET_{N-T} = \int \mathrm{E_t}(R)\mathrm{d}R / \int \mathrm{d}R \quad (11)$$

are summarized in Table 9. In PG only or PG–BuOH 1 : 2 solvent, the observed values of quenching efficiency by steady-state and time-resolved fluorescence measurement are slightly

**Table 9** Theoretical energy transfer efficiency between NpCD and trinitrophenyl unit in various solvents at 25 °C

| | NpCD–trinitrophenyl unit (%) | |
|---|---|---|
| | $ET_{N-T\ (277\ nm)}$ [a] | $ET_{N-T\ (327\ nm)}$ [b] |
| PG | 44.9 | 45.1 |
| PG–MeCN 1 : 2 | 42.1 | 41.8 |
| PG–BuOH 1 : 2 | 42.9 | 42.4 |
| PG–DMSO 1 : 2 | 37.5 | 36.1 |
| PG–formamide 1 : 2 | 43.0 | 42.9 |

[a] $ET_{N-T\ (277\ nm)} = \int E_{t\ (277\ nm)}(R)\, \mathrm{d}R / \int \mathrm{d}R$. [b] $ET_{N-T\ (327\ nm)} = \int E_{t\ (327\ nm)}(R)\, \mathrm{d}R / \int \mathrm{d}R$.

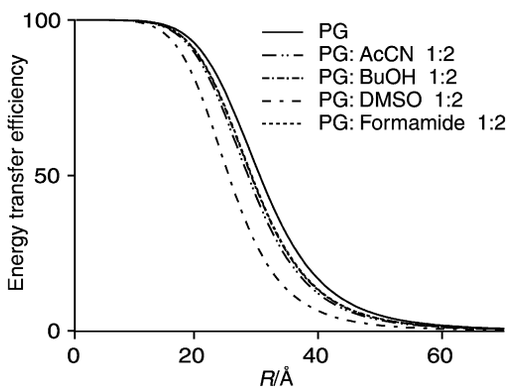


**Fig. 4** Theoretical energy transfer efficiency ($E_t$) between naphthalene and trinitrophenyl units in various solvents were calculated by the following equation: $E_t = R_0^6/R_0^6 + R^6$ where $R$ is the distance between naphthalene and trinitrophenyl units and $R_0$ is the Förster radius.

larger than the theoretical energy transfer efficiency, while in the other solvents, the experimental values are much smaller than the theoretical values. For example, although the theoretical energy transfer efficiencies in PG–BuOH 1 : 2 and PG–formamide 1 : 2 solvents are almost the same at $\lambda_{ex}$ 277 and 327 nm, the experimental quenching values in PG–BuOH 1 : 2 solvent are much larger than those in PG–formamide 1 : 2 solvent. These results also suggest that in the high relative permittivity dielectric constant ($\varepsilon$) solvents such as MeCN ($\varepsilon$ = 37.5), DMSO ($\varepsilon$ = 48.9), formamide ($\varepsilon$ = 111.0), the electron transfer is the dominant process to quench the naphthalene fluorescence, and the lifetime of the radical anion of the trinitrophenyl units generated by electron transfer may be so long that the following process was not allowed to occur before the recovery of the neutral trinitrophenyl units.

The Förster radius values between naphthalene and naphthalene in various solutions at excitation wavelength 277 nm are also summarized in Table 5, they are about twice the length of the α-CD height (7 Å). Thus, theoretically, energy migration between the naphthalene units can occur and facilitate the energy transfer to the trinitrophenyl units from the distant naphthalene units. Actually, the energy migration between the naphthalene units of **9**–**12** was observed more markedly than that of **8** by the anisotropy measurements in PG at −70 °C.

### Electron transfer mechanism

Fig. 5 shows the cyclic voltammetry pattern of TNP-PEG (Scheme 1) in MeCN; the observed value of the reduction potential [TNP/TNP$^{\bullet -}$] was −0.73 V. The observation that the anode current peak for redox of TNP radical anion was not clear means that the rate of electron transfer from TNP radical anion to the electrode is too fast for this scan speed to observe the redox peak. The oxidation potential of [NpCD$^{\bullet +}$/NpCD] may be beyond 1.5 V, so the accurate value could not be detected in our apparatus. We use an oxidation potential value of naphthalene [naphthalene$^{\bullet +}$/naphthalene] of 1.62 V in

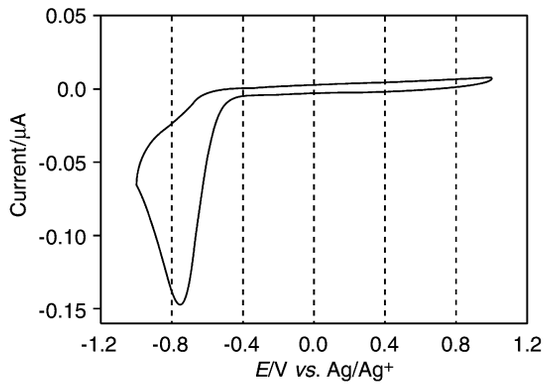


**Fig. 5** Cyclic voltammogram (sweep rate 100 mV $s^{-1}$) for TNP-PEG in MeCN at room temperature.

MeCN[23] when the oxidation potential of NpCD[$NpCD^{\bullet+}$/NpCD] is discussed. The free energy change ($\Delta G$) from a pair of the excited state donor *D and the ground state acceptor A to the pair of the oxidized donor $D^+$ and the reduced acceptor $A^-$ generated by electron transfer can be estimated by the eqn. (12),

$$\Delta G\,(\text{kcal mol}^{-1}) = nF\,[E^0(\text{D}^+/^*\text{D}) - E^0(\text{A}/\text{A}^-)] \quad (12)$$

where $n$ is the number of transferred electrons, $F$ is the Faraday constant (96493 C $mol^{-1}$). $E^0(D^+/^*D)$ and $E^0(A/A^-)$ are the redox potentials of the excited state donor and ground state acceptor, respectively. $D^+$, *D, A, and $A^-$ represent an oxidized donor, an excited state donor, a ground state acceptor, and a reduced acceptor, respectively. A redox potential for an excited state of the donor $E^0(D^+/^*D)$ can be calculated from the redox potential of the ground state of the donor using the zero–zero excitation energy ($E_{00}$), as shown in eqn. (13). The free energy change of the electron transfer ($\Delta G$) is given using eqn. (13) by the Rehm–Weller equation eqn. (14), where $w_p$ is the coulombic

$$E^0(\text{D}^+/^*\text{D}) = E^0(\text{D}^+/\text{D}) - E_{00} \quad (13)$$

$$\Delta G\,(\text{kcal mol}^{-1}) = nF[E^0(\text{D}^+/\text{D}) - E^0(\text{A}/\text{A}^-)] - E_{00} - w_p \quad (14)$$

stabilization energy of the product. However, there are two distinct intermediate states of the electron transfer process from a pair D* and A to the pair of $D^+$ and $A^-$: one is generated through the solvent separated ion pair (SSIP) and another is generated through the exciplex (EX).[23] The difference between these two intermediates is that the ion pair of oxidized $D^+$ and reduced $A^-$ generated through SSIP are divided completely and mediated by the solvent, and in that generated through EX, $D^+$ and reduced $A^-$ are contacted forming an exciplex. The solvent surrounds the $D^+$ and $A^-$ more easily with increasing relative permittivity of the solvents to stabilize these ion pairs and prevent back electron transfer. This means that the SSIP process is likely to occur. The above-mentioned Rehm–Weller equation can be modified by estimating the relative permittitvity of the solvent. If the electron transfer occurs through the solvent separated ion pair (SSIP) process, the free energy change $\Delta G_{SSIP}$ is given by eqn. (15), where 37.5 is the relative permittivity of

$$\Delta G_{SSIP}(\text{kcal mol}^{-1}) = 23.06[E^0(D^+/D) - E^0(A/A^-)]^{37.5} - E_{00} - 166\left(\frac{1}{r_D} + \frac{1}{r_A}\right)\left(\frac{1}{37.5} - \frac{1}{\varepsilon}\right) - \frac{332}{\varepsilon\, d_{cc}} \quad (15)$$

MeCN, $r_D$ and $r_A$ are the molecular radii of donor and acceptor, $d_{cc}$ is the distance between the centers of the donor and acceptor, $d_{cc} = r_D + r_A$, $\varepsilon$ is the relative permittivity of the

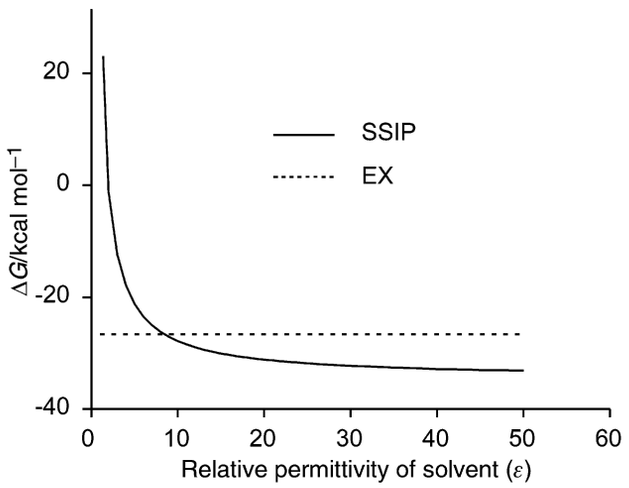


**Fig. 6** The free energy change of electron transfer through the SSIP process ($\Delta G_{SSIP}$) and through the EX process ($\Delta G_{EX}$) *versus* the relative permittivity of the solvent ($\varepsilon$).

solvent. If the electron transfer occurs through the exciplex process, the free energy change $\Delta G_{EX}$ is given by eqn. (16),

$$\Delta G_{EX}\,(\text{kcal mol}^{-1}) = 23.06[E^0(D^+/D) - E^0(A/A^-)]^{37.5} - E_{00} - \frac{\mu^2}{\rho^3}\left(\frac{\varepsilon - 1}{2\varepsilon + 1} - 4.3\right) + 8.8 \quad (16)$$

where $\mu$(debye) is the dipole moment of the exciplex intermediate, and $\rho$ is the radius of the exciplex complex. The $\mu^2/\rho^3$ term represents the solvation free energy of the exciplex. In these calculations, we use 2.5 Å for $r_D$ and $r_A$, 12 debye for $\mu$ and 5 Å for $\rho$.[23] The $E_{00}$ corresponds to the excitation energy at 327 nm, which is the absorption peak of NpCD at the highest wavelength, and this value is 87.4 kcal $mol^{-1}$. Fig. 6 shows the calculated $\Delta G_{SSIP}$ and $\Delta G_{EX}$ values *versus* the change of relative permittivity of the solvent. This suggests that in our polyrotaxanes, the EX process is rather favorable in the low dielectric solvents. This means that the back electron transfer easily occurs and the radical anion of the trinitrophenyl units may not be stabilized as much. With increasing relative permittivity of the solvent, the through SSIP process becomes more favorable, in which the trinitrophenyl radical anion is more stabilized by the solvent and the back electron transfer is effectively prevented. This means the lifetime of the radical anion becomes longer with increasing relative permittivity of the solvent.

## Conclusion

We constructed a polyrotaxane series as a light harvesting antenna model, which consist of various ratios of α-CD and NpCD threaded by a poly(ethylene glycol) chain bearing a trinitrophenyl unit at both ends. The quenching efficiency of the naphthalene unit ($QE$, $E_q$) was estimated by steady-state and time-resolved fluorescence spectroscopy. The observed results are rationalized by the combination of two processes; one is energy transfer to trinitrophenyl and the other is electron transfer, and the dominant factor in these processes depends on the solvent. The Förster mechanism was applied to analyze the energy transfer process. In the PG only, PG–BuOH 2 : 1 and 1 : 2 solvents, the energy transfer process is the main factor to quench the naphthalene fluorescence, and the rate constant of energy transfer $k_{ET}$ may be constant in all the polyrotaxanes **8**–**12**. There are discrepancies between these studies and the previously reported results, in which anthracene units were conjugated to both ends of the PEG chain instead of trinitrophenyl units. However, the Förster radius between the naphthalene and trinitrophenyl units in PG (30.7 Å, $\lambda_{ex}$ = 327 nm) is much larger

than that between the naphthalene and anthracene units (23 Å, $\lambda_{ex}$ = 327 nm). The energy migration between the naphthalene units was also suggested by glass-matrix anisotropy measurements and the Förster radius between naphthalenes (13.2 Å). In contrast, we consider the electron transfer process to quench the naphthalene fluorescence to be a main factor in PG–MeCN 1 : 2, PG–DMSO 1 : 2 and PG–formamide 1 : 2 solvents. In such solvents, the quenching efficiency decreases with increasing naphthalene content in the polyrotaxanes. This may be because the lifetime of the radical anion of the trinitrophenyl unit generated by the electron transfer is long enough to prevent the following quenching process, and relatively, the higher quenching efficiency was observed only in the low naphthalene content polyrotaxanes. The redox potentials of naphthalene units and trinitrophenyl units were measured by cyclic voltammetry in MeCN. These results suggest that electron transfer from the exited state naphthalene to trinitrophenyl units is thermodynamically favorable in all the solvents used in our experiments.

## Experimental

### Materials

α-CD was a kind gift from Nihon Shokuhin Kako Co., Ltd. Poly(oxyethylene)diamine (approximate MW = 2000) (diamino-PEG) was purchased from Scientific Polymer Products and was used without further purification.

### Measurements

$^1$H NMR spectra were recorded on a Varian VXR500S 500 MHz NMR spectrometer. Chemical shifts were referenced to those of the solvent values ($\delta$ 2.62 ppm for DMSO, 4.7 ppm for HOD, 7.28 ppm for $CDCl_3$). The UV–vis absorption spectra were recorded on a Shimadzu model UV-3100 spectrometer using 1-cm quartz cells. Fluorescence spectra were taken on a Hitachi Fluorescence Photometer F-2500. The fluorescence quantum yields of the samples were determined using quinine sulfate solution in 0.05 M $H_2SO_4$ ($\phi_n$ = 0.55) as the standard. Fluorescence and excitation spectra were corrected for the wavelength dependence of detector sensitivity and the excitation light source output. The spectra were recorded using a 1-cm quartz cell. Fluorescence lifetimes were measured on a time-correlated single photon counting fluorometer (Horiba NAES-550). A total of 10000 counts were collected in the maximum channel. The absorbances of the solutions were between 0.1 and 0.3 at the excitation wavelength. The fluorescence decay profile was analyzed by reconvolution of the instrumental response function and monoexponential or multiexponential decay of the emission using an iterative nonlinear least squares method. The goodness-of-fit was assessed using the plots of weighted residuals, reduced $\chi^2$ values, and Durbin–Watson parameters. Laser flash photolysis was carried out by using an Nd-YAG laser (Spectra Physics Quanta Ray DCR-3) with fourth-harmonic light of 266 nm at room temperature. A xenon arc lamp was used as a monitoring light beam. The transient spectra were stored in a strong oscilloscope (SONY-Tektronix 11401). Cyclic voltammetry (CV) was performed on a computerized automatic polarization system HZ-3000 (Hokuto Denko Co., Tokyo) in nitrogen-purged MeCN containing 100 mM $NaClO_4$ as supporting electrolyte at room temperature. A glassy carbon disk electrode (Ø 3 mm) was used as a working electrode with a platinum counter electrode and an $Ag/Ag^+$ reference electrode in a three-electrode system. The surface of the working electrode was polished with commercial Alpha Micropolish Alumina. The concentration of the compounds examined was 20 mM. The scan rate was 100 mV $s^{-1}$. Elemental analyses were performed by the Analytical Division of the Research Laboratory of Resources Utilization of Tokyo Institute of Technology.

### Synthesis of polypseudorotaxanes 1, 2, 3, 4, 5 and 6

The diamino-PEG (0.037 g, $1.83 \times 10^{-5}$ mol) was added into aqueous solutions (2 ml) A (α-CD; 0.450 g, $4.63 \times 10^{-4}$ mol), B (α-CD; 0.360 g, $3.70 \times 10^{-4}$ mol, NpCD; 0.107 g, $9.20 \times 10^{-5}$ mol), C (α-CD; 0.270 g, $2.78 \times 10^{-4}$ mol, NpCD; 0.215 g, $1.85 \times 10^{-4}$ mol), D (α-CD; 0.180 g, $1.85 \times 10^{-4}$ mol, NpCD; 0.322 g, $2.77 \times 10^{-4}$ mol), E (α-CD; 0.090 g, $9.25 \times 10^{-5}$ mol, NpCD; 0.430 g, $3.70 \times 10^{-4}$ mol), and diamino-PEG (0.031 g, $1.53 \times 10^{-5}$ mol) was added into the aqueous solution F (NpCD; 0.450 g, $3.87 \times 10^{-4}$ mol). After adding the diamino-PEG, white precipitates were formed in each solution. The precipitates were collected by centrifuge and then dried *in vacuo* (**1**, **2**, **3**, **4**, **5**, **6** from A, B, C, D, E, F solutions, respectively), giving **1** (0.40 g, $1.53 \times 10^{-5}$ mol, 83.1%), **2** (0.36 g, $1.66 \times 10^{-5}$ mol, 90.4%), **3** (0.34 g, $1.78 \times 10^{-5}$ mol, 96.9%), **4** (0.375 g, $1.76 \times 10^{-5}$ mol, 95.7%), **5** (0.33 g, $1.80 \times 10^{-5}$ mol, 92.0%), and **6** (0.25 g, $1.69 \times 10^{-5}$ mol, 92.0%). $^1$H NMR ($D_2O$): $\delta$ = 3.40–3.60 (12H; H-2,4 of α-CD of **1**, **2**, **3**, **4**, **5**, **6**), 3.65 (s, 7.3H, 9.2H, 10.8H, 10.2H, 12.6H, 16.3H; $CH_2$ of diamino-PEG of **1**, **2**, **3**, **4**, **5**, **6**, respectively), 3.70–4.00 (18H; H-3,5,6 of α-CD of **1**, **2**, **3**, **4**, **5**, **6**), 4.85–5.05 (6H; H-1 of α-CD of **1**, **2**, **3**, **4**, **5**, **6**), 7.70–8.20 (naphthyl peaks of **2**, **3**, **4**, **5**, **6**), 8.54 (s, 0.15H, 0.40H, 0.60H, 0.80H, 1.00H; H-1 of naphthalene of **2**, **3**, **4**, **5**, **6**, respectively).

### Synthesis of polyrotaxanes 7, 8, 9, 10, 11 and 12

Polypseudorotaxanes **1**, **2**, **3**, **4**, **5**, **6** (0.10 g) were merged in the pH 8.0 $KH_2PO_4$–NaOH buffer aqueous solution (5 ml) and then 2,4,6-trinitrobenzene-1-sulfonate (20.0 equivalent for amine) was added into these solutions while stirring rapidly. After 2 h, the solutions were centrifuged and then supernatant fluids were removed. Water was poured in again to wash the products. Then solutions were centrifuged and supernatant fluids were removed again. This process was repeated with water (at least 10 times) and with water containing a small amount of ethanol (0.1%, at least 5 times), and then the precipitates were dried in *vacuo* to obtain a yellow powder (**7**, **8**, **9**, **10**, **11**, **12** from **1**, **2**, **3**, **4**, **5**, **6**, respectively). Yield: **7** (17.0 mg, $9.06 \times 10^{-7}$ mol, 23.8%), **8** (29.2 mg, $1.71 \times 10^{-6}$ mol, 37.3%), **9** (34.8 mg, $1.99 \times 10^{-6}$ mol, 39.0%), **10** (18.1 mg, $1.20 \times 10^{-6}$ mol, 25.6%), **11** (15.6 mg, $1.08 \times 10^{-6}$ mol, 19.6%), **12** (14.0 mg, $9.96 \times 10^{-7}$ mol, 15.0%). $^1$H NMR (DMSO-$d_6$): $\delta$ = 3.00–4.00 (br, H-2, 3, 4, 5, 6 of α-CD of **7**, **8**, **9**, **10**, **11**, **12**), 3.48–3.52 (br, $CH_2$ of diamino-PEG of **7**, **8**, **9**, **10**, **11**, **12**), 4.42–4.44 (br, HO-6 of α-CD of **7**, **8**, **9**, **10**, **11**, **12**), 5.06–5.08 (br, H-1 of α-CD of **7**, **8**, **9**, **10**, **11**, **12**), 5.40–5.80 (br, HO-2, 3 of α-CD of of **7**, **8**, **9**, **10**, **11**, **12**), 7.60–9.00 (br, naphthyl peaks of **8**, **9**, **10**, **11**, **12**); elemental analysis calcd (%) for **7** $C_{667.2}H_{1128}O_{527}N_8$: C 45.29, H 6.43, N 0.63; found: C 44.97, H 6.27, N 0.67%; calcd for **8** $C_{627.8}H_{1030.8}O_{475.6}N_8S_{3.8}$: C 45.91, H 6.32, N 0.68, S 0.74; found: C 46.18, H 6.51, N 0.68, S 0.56%; calcd for **9** $C_{570.2}H_{916.2}O_{416.4}N_8S_{4.7}\cdot 7(H_2O)$: C 46.20, H 6.33, N 0.76, S 1.01; found: C 45.96, H 6.31, N 0.66, S 0.94%; calcd for **10** $C_{576.4}H_{908.4}O_{410.8}N_8S_{6.4}\cdot 12(H_2O)$: C 46.32, H 6.29, N 0.75, S 1.37; found: C 45.97, H 6.14, N 0.66, S 1.25%; calcd for **11** $C_{564}H_{866.4}O_{387.8}N_8S_{8.4}$: C 47.59, H 6.14, N 0.79, S 1.89; found: C 47.74, H 6.07, N 0.88, S 2.03%; calcd for **12** $C_{557.4}H_{839.4}O_{372.8}N_8S_{9.9}$: C 48.04, H 6.07, N 0.80, S 2.28; found: C 48.28, H 6.23, N 0.99, S 2.11%.

## References


1 (*a*) R. van Grondella and O. J. G. Somsen, *Excitation energy transfer in photosynthesis in Resonance Energy Transfer*, Eds. D. L. Andres and A. A. Demidov, John Wiley & Sons, Chichester, 1999, pp. 366–398; (*b*) Govindjee, J. Barber, W. A. Cramer, J. H. C. Goedheer, J. Lavorel, R. Marcelle and B. Zilinskas, *Excitation Energy and Electron Transfer in Photosynthesis*, Marinus Nijhoff Publishers, Dordrecht, 1987.

2 L. A. Staehelin (Chloroplast Structure and Supramolecular Organization of Photosynthetic Membranes), K. Sauer (Photosynthetic Light Reactions–Physical Aspects), J. P. Thornber (Biochemical Characterization and Structure of Pigment-Proteins of Photosynthetic Organisms), D. R. Ort (Energy Transduction in Oxygenic Photosynthesis: an Overview of Structure and Mechanism), P. L. Dutton (Energy Transduction in Anoxygenic Photosynthesis), H. Zuber, R. J. Cogdell, E. Gantt, J. M. Anderson and J. Barrett (Comparative Biochemistry of Light-Harvesting Systems), R. S. Knox, A. R. Holzwarth, N. E. Geacintov, J. Breton and H. Scheer (Trapping Events in Light-Harvesting Assemblies), W. W. Parson, D. Holten, D. M. Tiede, J. R. Norris, G. van Brakel, H. Michael, J. Deisenhofer, J. E. Hearst, R. E. Blankenship, R. C. Fuller and A. J. Hoff (Physical Determinants of Charge Separation Processes), B. A. Diner, C. F. Yocum, B. Andersson, C. J. Arntaen, H. B. Pakrasi, D. J. Kylne, I. Ohad, P. Sétif, P. Mathis and F.-A. Wollman (Photosystem I and II: Structure, Proteins, and Cofactors), G. Hauska, J. Whitmarch, P. Joliot, A. Joliot, R. C. Prince, W. Haehnel, B. A. Melandri, R. A. Dilley, R. E. McCarty, C. M. Nalin, H. Strotmann, G. Sandmann and P. Böger (Energy Transfer and Energy-Coupling Processes), in *Encyclopedia of Plant Physiology, vol. 19, Photosynthesis III, Photosynthetic Membranes and Light Harvesting Systems*, Eds. L. A. Staehelin and C. J. Arntzen, Springer-Verlag, Berlin, 1986, pp. 1–602.

3 (*a*) R. H. Schmehl and D. G. Whitten, *J. Am. Chem. Soc.*, 1980, **102**, 1938; (*b*) O. Mongin, N. Hoyler and A. Gossauer, *Eur. J. Org. Chem.*, 2000, 1193; (*c*) Y. Itoh, M. Nakada, H. Satohh, A. Hachimori and S. E. Webber, *Macromolecules*, 1993, **26**, 1941; (*d*) M. Kuragaki and M. Sisido, *J. Phys. Chem.*, 1996, **100**, 16019.

4 (*a*) M. A. Fox and P. F. Birtt, *J. Phys. Chem.*, 1990, **94**, 6351; (*b*) F. Bai, C.-H. Chang and S. E. Webber, *Macromolecules*, 1986, **19**, 2484; (*c*) W. E. Jones, Jr., S. M. Baxter, G. F. Strouse and T. J. Meyer, *J. Am. Chem. Soc.*, 1993, **115**, 7363; (*d*) L. M. Dupray, M. Devenny, E. R. Striplin and T. J. Meyer, *J. Am. Chem. Soc.*, 1997, **119**, 10243.

5 (*a*) J. S. Aspler, C. E. Hoyle and J. E. Guillet, *Macromolecules*, 1978, **11**, 925; (*b*) D. Ng and J. E. Guillet, *Macromolecules*, 1982, **15**, 724; (*c*) D. Ng and J. E. Guillet, *Macromolecules*, 1982, **15**, 728.

6 (*a*) L. A. J. Chrisstoffels, A. Adronov and J. M. J. Fréchet, *Angew. Chem., Int. Ed.*, 2000, **39**, 2163; (*b*) S. L. Gilat, A. Adronov and J. M. J. Fréchet, *Angew. Chem., Int. Ed.*, 1999, **38**, 1422; (*c*) D.-L. Jiang and T. Aida, *J. Am. Chem. Soc.*, 1998, **120**, 10895; (*d*) V. Balzani, S. Campagna, G. Denti, A. Juris, S. Serroni and M. Venture, *Acc. Chem. Res.*, 1998, **31**, 26; (*e*) B. Schlicker, P. Belser, L. DeCola, E. Sabbioni and V. Balzani, *J. Am. Chem. Soc.*, 1999, **121**, 4207.

7 (*a*) A. Bar-Haim, J. Klafter and R. Kopelman, *J. Am. Chem. Soc.*, 1997, **119**, 6197; (*b*) A. Bar-Haim and J. Klafter, *J. Lumin.*, 1998, **76&77**, 197; (*c*) C. Devadoss, P. Bharathi and J. S. Moore, *J. Am. Chem. Soc.*, 1996, **118**, 9635; (*d*) M. R. Shortreed, S. F. Swallen, Z.-Y. Shi, W. Tan, Z. Xu, C. Devadoss, J. S. Moore and R. Kopelman, *J. Phys. Chem. B*, 1997, **101**, 6318; (*e*) R. Kopelman, M. Shortreed, Z.-Y. Shi, W. Tan, Z. Xu, J. S. Moore, A. Bar-Haim and J. Klafter, *Phys. Rev. Lett.*, 1997, **78**, 1239.

8 (*a*) S.-I. Kawahara, T. Uchimaru and S. Murata, *Chem. Commun.*, 1999, 563; (*b*) E. Ishow, A. Credi, V. Balzani, F. Spadola and L. Mandolini, *Chem. Eur. J.*, 1999, **5**, 984; (*c*) T. Morita, S. Kimura and Y. Imanighi, *J. Am. Chem. Soc.*, 1999, **121**, 581.

9 (*a*) T. Morita, S. Kimura and Y. Imanishi, *J. Phys. Chem. B*, 1997, **101**, 4536; (*b*) K. Iida, M. Nango, M. Matsuura, M. Yamaguchi, K. Sato, K. Tanaka, K. Akimoto, K. Yamashita, K. Tsuda and Y. Kurono, *Langmuir*, 1996, **12**, 450; (*c*) M. Nango, T. Hikita, T. Nakano, T. Yamada, M. Nagata, Y. Kurono and T. Ohtsuka, *Langmuir*, 1998, **14**, 407.

10 (*a*) S. Serroni, S. Campagna, R. P. Nascone, G. S. Hanan, G. J. E. Davidson and J.-M. Lehn, *Chem. Eur. J.*, 1999, **5**, 3523; (*b*) R. A. Haycock, A. Yartsev, U. Michelsen, V. Sundström and C. A. Hunter, *Angew. Chem., Int. Ed.*, 2000, **39**, 3616; (*c*) F. Barigelletti, L. Flamigni, V. Balzani, J.-P. Collin, J.-P. Sauvage, A. Sour, E. C. Constable and A. M. W. C. Thompson, *J. Am. Chem. Soc.*, 1994, **116**, 7692.

11 Y.-Z. Hu, S. H. Bossmann, D. van Loyen, O. Schwarz and H. Dürr, *Chem. Eur. J.*, 1999, **5**, 1267.

12 (*a*) J.-P. Collin, P. Gaviña, V. Heitz and J.-P. Sauvage, *Eur. J. Inorg. Chem.*, 1998, 1; (*b*) M. Linke, J.-C. Chambron, V. Heitz and J.-P. Sauvage, *J. Am. Chem. Soc.*, 1997, **119**, 11329; (*c*) M. Andersson, M. Linke, J.-C. Chambron, J. Davidsson, V. Heitz, J.-P. Sauvage and L. Hammarström, *J. Am. Chem. Soc.*, 2000, **122**, 3526; (*d*) J.-C. Chambron and J.-P. Sauvage, *Chem. Eur. J.*, 1998, **4**, 1362; (*e*) A. C. Benniston, *Chem. Soc. Rev.*, 1996, 427.

13 (*a*) V. Balzani and F. Scandola, *Photochemical and Photophysical Devices*, in *Comprehensive Supramolecular Chemistry, vol. 10*, Eds. J. L. Atwood, J. E. D. Davies, D. D. Macnicol, F. Vögtle, J.-M. Lehn and D. N. Reinhoudt, Pergamon, Oxford, 1996, pp. 687–746; (*b*) M. D. Ward, *Chem. Soc. Rev.*, 1997, **26**, 365; (*c*) Y.-Z. Hu, S. Tsuki, S. Shinkai, S. Oishi and I. Hamachi, *J. Am. Chem. Soc.*, 2000, **122**, 241; (*d*) Y.-Z. Hu, S. Tsuki, S. Shinkai, S. Oishi and I. Hamachi, *Chem. Eur. J.*, 2000, **6**, 1907; (*e*) G. Steinberg-Yfrach, P. A. Liddel, S.-C. Hung, A. L. Moore, D. Gust and T. A. Moore, *Nature*, 1997, **385**, 239; (*f*) G. Steinberg-Yfrach, J.-L. Rigaud, E. N. Durantini, A. L. Moore, D. Gust and T. A. Moore, *Nature*, 1998, **392**, 479.

14 (*a*) M. Tamura and A. Ueno, *Chem. Lett.*, 1998, **369**, 198; (*b*) M. Tamura and A. Ueno, *Bull. Chem. Soc. Jpn.*, 2000, **73**, 147.

15 M. Tamura, D. Gao and A. Ueno, *Chem. Eur. J.*, 2001, **7**, 1390.

16 (*a*) A. Harada, J. Li and M. Kamachi, *Nature*, 1992, **356**, 325; (*b*) A. Harada, *Coord. Chem. Rev.*, 1996, **148**, 115; (*c*) A. Harada, J. Li and M. Kamachi, *J. Am. Chem. Soc.*, 1994, **116**, 3192.

17 A. Harada, J. Li and M. Kamachi, *Chem. Commun.*, 1997, 1413.

18 N. J. Turro, *Modern Molecular Photochemistry*, The Benjamin/Cummings Publishing Company, Inc., 1978, p. 296.

19 (*a*) A. A. Lamola and N. J. Turro, *Energy Transfer and Organic Photochemistry*, in *Techniques of Organic Chemistry*, Eds. P. A. Leermakers and A. Weissberger, Interscience Publishers, New York, 1969, vol. XIV, pp. 20–72; (*b*) R. Kopelman, M. Shortreed, Z.-Y. Shi, W. Tan, Z. Xu, J. S. Moore, A. Bar-Haim and J. Klafter, *Phys. Rev. Lett.*, 1997, **78**, 1239.

20 (*a*) H. Murakami, T. Hohsaka, Y. Ashizuka and M. Sisido, *J. Am. Chem. Soc.*, 1998, **120**, 7520; (*b*) M. Sisido, *Adv. Photochem.*, 1997, **22**, 197.

21 A. M. Fremenko, V. P. Kondilenko, O. I. Yakimova, V. Ya. Cherny and A. A. Chuiko, *J. Mol. Struct.*, 1992, **267**, 309.

22 G. J. Kavarons, *Fundamentals of Photoinduced Electron Transfer*, Wiley-VCH, New York, 1997, Ch. 1 and 2.

23 (*a*) D. M. Gravett and J. E. Guillet, *J. Am. Chem. Soc.*, 1993, **15**, 5970; (*b*) M. N. Berberan-Santos, P. Choppinet, A. Fedorov, L. Jullien and B. Valeur, *J. Am. Chem. Soc.*, 1999, **121**, 2526.

24 S. E. Webber, *Photochem. Photobiol.*, 1997, **65**, 33.